Journal of Bone and Mineral Metabolism (2019) 37:212–223
https://doi.org/10.1007/s00774-018-0919-y

ORIGINAL ARTICLE

High calcium, phosphate and calcitriol supplementation leads to an osteocyte-like phenotype in calcified vessels and bone mineralisation defect in uremic rats

Sarah-Kim Bisson[1] · Roth-Visal Ung[1] · Sylvain Picard[1] · Danika Valade[1] · Mohsen Agharazii[1] · Richard Larivière[1] · Fabrice Mac-Way[1]

Received: 5 July 2017 / Accepted: 20 February 2018 / Published online: 30 March 2018

Abstract

A link between vascular calcification and bone anomalies has been suggested in chronic kidney disease (CKD) patients with low bone turnover disease. We investigated the vascular expression of osteocyte markers in relation to bone microarchitecture and mineralization defects in a model of low bone turnover CKD rats with vascular calcification. CKD with vascular calcification was induced by 5/6 nephrectomy followed by high calcium and phosphate diet, and vitamin D supplementation (Ca/P/VitD). CKD + Ca/P/VitD group ($n = 12$) was compared to CKD + normal diet ($n = 12$), control + normal diet ($n = 8$) and control + Ca/P/VitD supplementation ($n = 8$). At week 6, tibia, femurs and the thoracic aorta were analysed by Micro-Ct, histomorphometry and for expression of osteocyte markers. High Ca/P/VitD treatment induced vascular calcification only in CKD rats, suppressed serum parathyroid hormone levels and led to higher sclerostin, DKK1 and FGF23 serum levels. Expression of sclerostin, DKK1 and DMP1 but not FGF23 were increased in calcified vessels from CKD + Ca/P/VitD rats. Despite low parathyroid hormone levels, tibia bone cortical thickness was significantly lower in CKD + Ca/P/VitD rats as compared to control rats fed a normal diet, which is likely the result of radial growth impairment. Finally, Ca/P/VitD treatment in CKD rats induced a bone mineralization defect, which is likely explained by the high calcitriol dose. In conclusion, Ca/P/VitD supplementation in CKD rats induces expression of osteocyte markers in vessels and bone mineralisation anomalies. Further studies should evaluate the mechanisms of high dose calcitriol-induced bone mineralisation defects in CKD.

Keywords Renal osteodystrophy · Vascular calcification · Bone · Osteocyte · Mineralisation defects

Introduction

The anomalies of bone, mineral and vascular calcification characterize the chronic kidney disease-mineral and bone disorder (CKD-MBD), and define the bone-vessels axis anomalies that typically affect CKD patients [1, 2]. On one hand, vascular calcification is now recognized as a highly regulated process where there is a trans-differentiation of vascular smooth muscle cells into osteoblast-like cells (bone forming cells) that mainly occurs in CKD and diabetes population [3, 4]. On the other hand, bone disorders in CKD are characterized by anomalies of bone mass, turnover and mineralisation that predispose to bone fragility [5, 6]. Both vascular and bone anomalies contribute to the high burden of bone fractures, cardiovascular morbidity and mortality in the CKD population [7–10].

In the last 15 years, treatment of high bone turnover (secondary hyperparathyroidism) with calcium and calcitriol may have contributed to the over-suppression of parathyroid hormone (PTH) and the development of low bone turnover disease in CKD patients [11]. Indeed, the prevalence of low bone turnover or adynamic bone disease (ABD) has been steadily increasing with a prevalence range from 5 to 40% in pre-dialysis and from 10 to 50% in dialysis patients [12, 13]. ABD has then been associated with development

Electronic supplementary material The online version of this article (https://doi.org/10.1007/s00774-018-0919-y) contains supplementary material, which is available to authorized users.

✉ Fabrice Mac-Way
fabrice.mac-way@mail.chuq.qc.ca

[1] Endocrinology and Nephrology Axis, Faculty and Department of Medicine, L'Hôtel-Dieu de Québec Hospital, CHU de Québec Research Center, Université Laval, 10 McMahon, Quebec City, QC G1R 2J6, Canada

of vascular calcification in CKD population [14, 15], but the pathophysiological mechanisms underlying this bone-vessels axis anomalies remain unknown [12].

Recently, osteocytes, the most abundant cells in the bone, have emerged as important actors in CKD-MBD. In addition to fibroblast growth factor 23 (FGF-23) and dentin matrix acidic phosphoprotein 1 (DMP1), new osteocyte markers have been suggested to be involved in the development of CKD-MBD. These include sclerostin and Dickkopf-related protein 1 (DKK1), which are highly expressed by the osteocytes and are known inhibitors of bone formation through repression of the Wnt/β-catenin pathway. These proteins could play a role in the development of ABD and vascular calcification in CKD [16–19], but how they could lead to the development of CKD-MBD in the context of low bone turnover is currently unknown.

Using the same model of CKD rats with vascular calcification as we previously reported [20, 21], the objectives of this study were: (1) to evaluate whether calcified vessels from CKD rats with low bone turnover disease express osteocytes markers and proteins that could affect bone metabolism and (2) to determine the anomalies of bone microarchitecture and mineralisation in relation to vascular calcification. We show that vascular calcification is associated with increased expression of osteocyte markers and decreased Wnt activation in the vessels. We also show that CKD animals with vascular calcification develop a bone mineralization defect, which is likely explained by the high dose of calcitriol supplementation.

Materials and methods

Animal experiments

The animal protocol was conducted in accordance with the guidelines of the Canadian Council of Protection of Animals and was approved by the local Animal Care Committee. Male Wistar rats weighing 200–225 g were purchased from Charles River (Saint-Constant, Quebec, Canada) and were allowed free access to standard rat chow and tap water in temperature and humidity control conditions with a 12-h dark/light cycle. CKD was induced by renal mass reduction with 5/6 nephrectomy as previously performed [20, 21]. Low bone turnover with low PTH and vascular calcification were induced by a high calcium (1.2%) and phosphate (1.2%) diet (Harlan Teklab, Madison, WI, USA), combined with 1,25-dihydroxyvitamin D3 subcutaneous injections (0.5 µg/kg 3 times per week) (Ca/P/VitD). Four groups of animals were studied: (1) control + normal chow ($n = 8$); (2) control + Ca/P/VitD ($n = 8$); (3) CKD + normal chow ($n = 12$) and; (4) CKD + Ca/P/VitD ($n = 12$). The animals were sacrificed after 4–6 weeks according to the health status of CKD + Ca/P/VitD rats. Before sacrifice, a 24-h urine sample was collected using individual metabolic cages. In order to evaluate the bone dynamic parameters, intraperitoneal tetracycline injections were given to all rats at two different periods (first dose at 50 mg/kg and second dose at 20 mg/kg), 5 days apart. The animals were anesthetized with isoflurane, exsanguinated, and serum was collected and frozen for biochemical analyses. The thoracic aorta, tibiae and femurs were harvested and fixed in buffered formalin for histological analysis or snap frozen and kept at − 80 °C until extraction for qRT-PCR and western blot analysis.

Biochemical parameters and mineral metabolism

Serum calcium, phosphorus, creatinine, urea, and urinary calcium, phosphorus and creatinine concentrations were determined with an autoanalyzer system (Ilab 1800, Lexington, MA, USA). Serum intact PTH and FGF23 (Immunotopics, San Clemente, CA, USA), total sclerostin (R&D Systems, Minneapolis, MN, USA) and DKK1 levels (Enzo Life Sciences, Farmingdale, NY, USA) were determined with ELISA kits according to the manufacturer's protocol.

Quantification of vascular calcification with Von Kossa staining

The thoracic aorta was fixed for 24 h, dehydrated and embedded in paraffin as previously described [20, 21]. Five µm thick sections were deparaffinized and rehydrated before staining for arterial calcification with 5% silver nitrate and light exposure, followed with 5% sodium thiosulfate, and counterstained with nuclear fast red. Quantification was performed on three different fields at magnification of 20× using the ImagePro-Plus analysis software (Media Cybernetics, Silver Spring, MD, USA).

Immunofluorescence and qRT-PCR analysis of Wnt inhibitors and Wnt ligands in vessels and bone

Immunofluorescence analysis of the thoracic aorta was performed as previously reported [20]. Briefly, 5 µm thick sections of paraffin-embedded aorta were deparaffinized and rehydrated. The heat-induced epitope retrieval method was used to unmask the antigens and the tissues were incubated in blocking serum (10% fetal bovine serum in phosphate buffered saline). The slides were incubated overnight with primary antibodies against DKK1 (Abcam, Cambridge, MA, USA), FGF23 (Bioss, Woburn, MA, USA), DMP1 (LifeSpan Biosciences, Seattle, WA, USA) or sclerostin (Biorbyt, Cambridge, UK). They were then washed in PBS before incubation with alexa fluor 594 anti-rabbit or anti-mouse secondary antibodies (Invitrogen, Waltham, MA, USA). Fluorescence images were examined at 20× magnification and

quantified using the ImagePro-Plus analysis software (Media Cybernetics, Rockville, MD, USA). For qRT-PCR analysis, bone marrow was first flushed out from the femur by centrifugation. Aortas and bones were then put in TRIzol reagent (Life Technologies, Waltham, MA, USA) and crushed using a Precellys 24 homogenizer equipped with a Cryolys cooler (Bertin Technologies, Montigny-Le-Bretonneux, France). qRT-PCR gene expression analysis was performed on a Stratagene Mx3005P (Agilent Technologies, Santa Clara, CA, USA) qRT-PCR system using Perfecta SYBR Green SuperMix, low ROX (Quanta Biosciences, Gaithersburg, MD, USA) with primers designed using NCBI Primer Blast algorithm (blast.ncbi.nlm.nih.goc/Blast.cgi, Online resource 1). Gene of interest expression, relative to three reference genes (B2m, Hprt1 and EEf1a1), was calculated based on the threshold cycle (C_t) using the Pfaffl formula [22].

Western blot analysis of Wnt pathway in vessels

To better evaluate the components of the Wnt pathway, protein expression of glycogen synthase kinase 3 (GSK-3β) and β-catenin were assessed in the thoracic aorta. The thoracic aorta proteins were extracted using TRIzol (Life Technologies, Waltham, MA, USA) and were kept in Laemmli Buffer 2× until SDS-PAGE analysis in Tris–Glycine Buffer. Primary antibodies against GSK-3β, phopho-GSK-3β (ser9), β-catenin and phospho-β-catenin (ser33/37) (Cell Signaling technology, Danvers, MA, USA) were used for immunodetection (LI-COR Biosciences, Lincoln, NE, USA). GAPDH (Novus Biologicals, Littleton, CO, USA) was used as sample normalization protein. Differences in protein concentration were quantified in Odyssey Imager (LI-COR Biosciences, Lincoln, NE, USA).

Assessment of bone cortical microarchitecture

Tibiae bone of each rat were scanned in a Micro-CT scanner (eXplore Locus, GE Healthcare Canada) at a resolution of 27 µm. Images analysis allowed the evaluation of cortical bone parameters: cortical volume, area, bone mineral density, bone mineral content, thickness, inner and outer perimeter using an automatic bone analysis software (eXplore MicroView from GE Healthcare, Canada).

Bone histomorphometry analysis

The tibia bone specimens were fixed in 70% ethanol, dehydrated in acetone and embedded in pure methyl methacrylate at low temperature as described by Chappard et al. [23]. Four non-serial 5 µm thick sections were cut on each tibia using a Microm-355S microtome (Rankin Biomedical Corporation, MI, USA). The sections remained unstained or stained with modified Goldner's trichrome for measurement of dynamic and static parameters, respectively, using a semi-automated image analysis system (Bioquant Meg IV System; R & M Biometrics, TE, USA) and a SummaSketch II (Summagraphics, Austin, TX, USA) digitizing tablet in conjunction with an Olympus BX45 microscope (Olympus, Richmond Hill, ON, Canada) and Infinity 2-2C CCD color camera (Lumenera Corporation, Ottawa, ON, Canada). All results were derived from two-dimensional primary measurements (tissue volume or area, bone volume or area and bone surface) performed in the secondary spongiosa. In order to take into account the potential effect of age on bone parameters, the primary spongiosa and the growth plate thickness were measured in all rats. All the abbreviations used are as proposed by the ASBMR Histomorphometry Nomenclature Committee [24, 25].

Data analysis

The results are expressed as means ± SEM. Values were compared using Kruskal–Wallis followed by Mann–Whitney *U* tests using the SPSS program (SPSS, Chicago, IL, USA). Spearman's rank correlation was used to assess the association between vascular calcification and mRNA transcript levels, bone microarchitecture and histomorphometry parameters. A value of $p < 0.05$ was considered statistically significant.

Results

Kidney function and mineral metabolism

Serum and urinary parameters are shown in Table 1. As expected, serum creatinine and urea were higher whereas creatinine clearance was lower in CKD rats as compared to control groups. Urinary phosphate was also increased in rats supplemented with Ca/P/VitD. This probably explains why serum calcium and phosphate were comparable between groups except for the CKD + Ca/P/VitD group in which creatinine clearance was further declined. As expected, PTH level was significantly diminished in both control and CKD rats supplemented with Ca/P/VitD.

Vascular calcification develops only in CKD + Ca/P/VitD rats

Extensive media vascular calcification assessed by Von Kossa staining was detected only in CKD + Ca/P/VitD showing 5.79% of calcification in thoracic aorta's surface (Fig. 1). None of the other experimental groups developed vascular calcification in the thoracic aorta.

Table 1 Biochemical parameters between groups

	CTL ($n=8$)	CTL + Ca/P/vitD ($n=8$)	CKD ($n=12$)	CKD + Ca/P/vitD ($n=12$)
Serum urea (mmol/L)	7.2 ± 0.4	7.3 ± 0.3	14.8 ± 0.4[a]	14.2 ± 1.4[a]
Serum creatinine (µmol/L)	22.6 ± 1.2	18.6 ± 1.0	49.3 ± 2.6[a]	70.1 ± 3.9[a,b]
Creatinine clearance (mL/min)	5.0 ± 0.6	5.9 ± 0.3	1.9 ± 0.1[a]	1.0 ± 0.1[a,b]
Serum phosphate (mmol/L)	2.25 ± 0.15	1.99 ± 0.08	2.21 ± 0.06	2.74 ± 0.18[a,b]
Serum calcium (mmol/L)	2.44 ± 0.04	2.39 ± 0.02	2.45 ± 0.03	2.45 ± 0.09
Urinary calcium (mg/d)	0.027 ± 0.004	0.181 ± 0.074	0.068 ± 0.009	0.142 ± 0.033
Urinary phosphate (mg/d)	0.833 ± 0.081	3.547 ± 0.284[c]	0.878 ± 0.099[a]	2.200 ± 0.153[a,b]
Serum PTH (pg/mL)	312 ± 56	61 ± 6[b,c]	378 ± 43	13 ± 3[b,c]
Serum sclerostin (pg/mL)	294 ± 15	324 ± 37	363 ± 26	758 ± 58[a,b]
Serum DKK1 (pg/mL)	407 ± 227	406 ± 26	570 ± 48[a,b]	1281 ± 136[a,b,c]
Serum FGF-23 (pg/mL)	515 ± 156	1159 ± 267	789 ± 166	37397 ± 3198[a,b,c]

Values are expressed as mean ± SD

CKD chronic kidney disease, *CTL* control, *Ca/P/VitD* calcium, phosphorus and vitamin D supplementation, *DKK1* Dickkopf-related protein 1, *FGF-23* fibroblast growth factor-23, *PTH* parathormone

[a] $p < 0.05$ vs. CTL and CTL + Ca/P/VitD

[b] $p < 0.05$ vs. CKD

[c] $p < 0.05$ vs. CTL

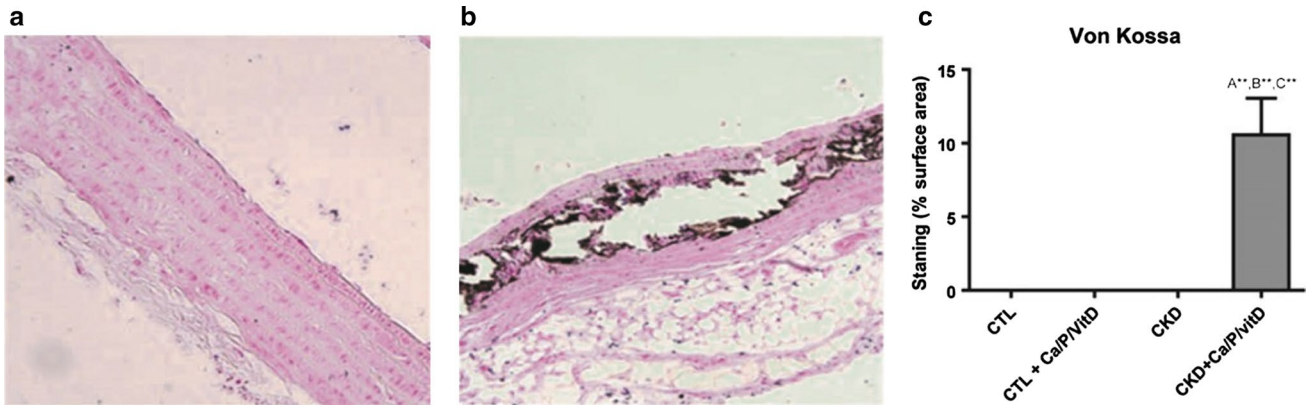

Fig. 1 Vascular calcification in the thoracic aorta. Von Kossa staining showing extensive media calcification of thoracic aorta only in CKD + Ca/P/VitD rats. **a** Representative image of vessels from control groups and CKD rats fed with normal diet showing no aortic calcification; **b** CKD rats with Ca/P/VitD supplementation showing extensive thoracic aorta calcification; **c** quantification of vascular calcification by Von Kossa in the different groups. *CKD* chronic kidney disease, *Ca/P/Vit D* calcium, phosphorus and vitamin D supplementation. **A****, **B****, **C****, $p < 0.001$ vs CTL, CTL + Ca/P/VitD and CKD, respectively

Increased vascular expression of sclerostin, DKK1 and DMP1, and serum levels of sclerostin, DKK1 and FGF23 in CKD + Ca/P/VitD rats

Immunofluorescence analysis from the thoracic aortas revealed that both sclerostin, DKK1 and DMP1 but not FGF23 expression were significantly increased in CKD + Ca/P/VitD rats as compared to the other groups (Fig. 2). In agreement with their vascular expression, serum sclerostin and DKK1 levels were also significantly elevated in CKD + Ca/P/VitD rats (Table 1).

Wnt signalling components in the vessel

Analysis of the Wnt pathway components in the thoracic aorta indicated that both total and phosphorylated β-catenin (ser33/37) were decreased in CKD rats given either normal or high Ca/P/VitD supplementation as compared to control groups (Fig. 3). Phosphorylated GSK-3β (ser9), which is inactive and cannot lead to β-catenin degradation, was decreased only in CKD supplemented with high Ca/P/VitD. These results suggest that there is suppression of the Wnt pathway in the vessels in CKD animals with vascular calcification. This is further supported

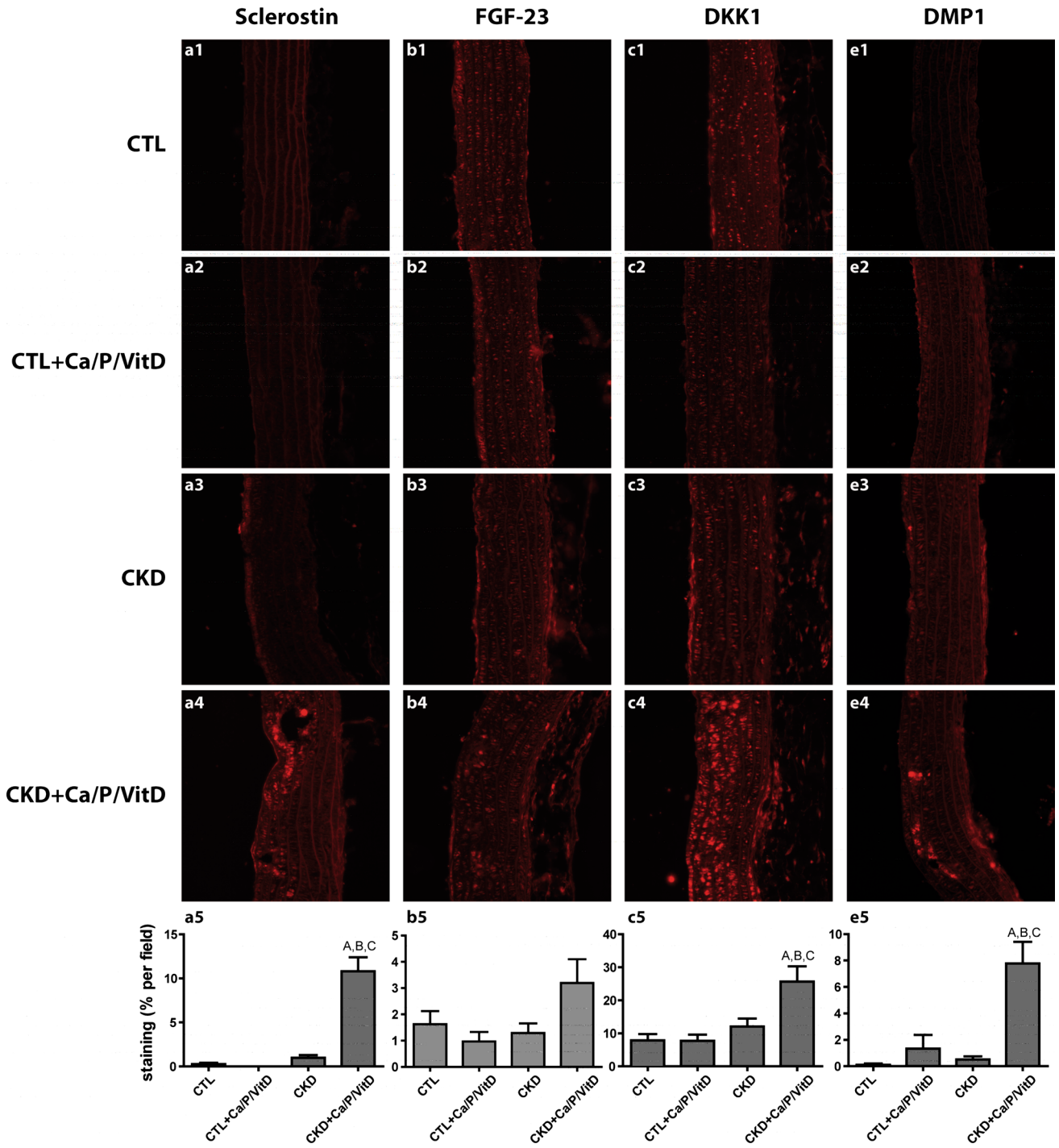

Fig. 2 Immunofluorescence analysis of osteocytes markers in the thoracic aorta. There is increased expression of sclerostin (a4 and a5), DKK1 (c4 and c5) and DMP1 (e4 and e5) in the thoracic aortas of CKD + Ca/P/VitD rats as compared to the other groups. FGF23 expression (b5) is higher but not statistically significant. CKD: chronic kidney disease; CTL: control; Ca/P/VitD: calcium, phosphorus and vitamin D supplementation. A, B, C, $p < 0.05$ vs CTL, CTL + Ca/P/VitD and CKD, respectively

by a decreased vascular transcription of AXIN2, which is a Wnt target gene, in the group with vascular calcification (Online resource 2). Transcript levels of several Wnt ligands (WNT3A, WNT5A, WNT10B, WNT11) and Fzd receptors (FZD1, FZD3, FZD7, FZD9) did not show differences between groups (Online resource 2). However, the severity of vascular calcification negatively correlated

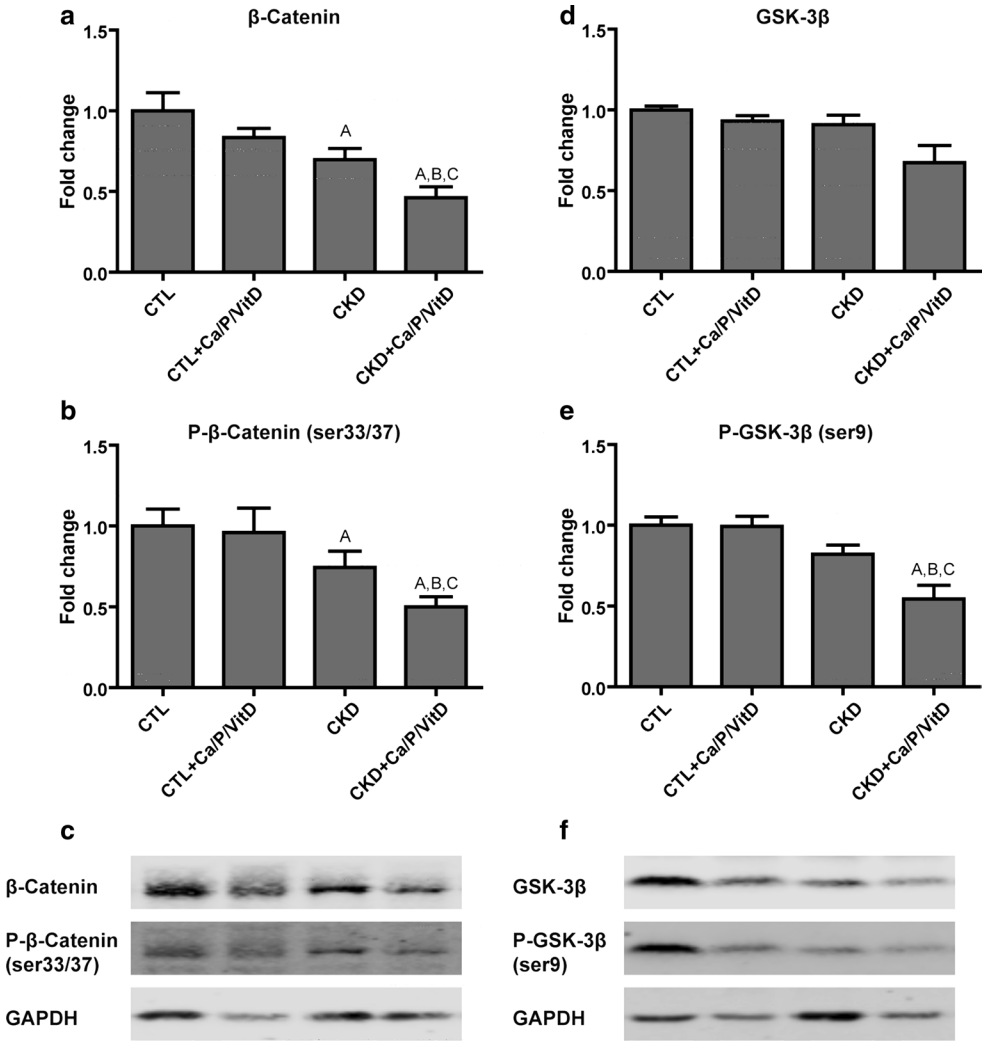

Fig. 3 Proteins expression of Wnt signalling pathway in thoracic aortas. Total and Ser33/37-phosphorylated β-catenin (**a**–**c**), total and Ser 9-phosphorylated GSK-3β (**d**–**f**). Both protein levels of total and phosphorylated β-catenin are decreased in CKD and CKD + Ca/P/VitD while only the phosphorylated GSK-3β is decreased in CKD + Ca/P/VitD animals. The decreased expression of phosphorylated GSK-3β suggests that there is suppression of the Wnt pathway alongside the increase in Wnt inhibitors in the calcified vessels. Each lane represents one rat and 4 images of blots each containing a maximum of 14 lanes were analyzed to calculate fold change. *CKD* chronic kidney disease, *CTL* control, *Ca/P/VitD* calcium, phosphorus and vitamin D supplementation. A, B, C, $p < 0.05$ vs CTL, CTL + Ca/P/VitD and CKD, respectively

with expression of WNT5A ($R - 0.680$, $p = 0.005$) and Wnt receptor FZD7 ($R - 0.622$, $p = 0.013$).

Cortical bone parameters are abnormal in CKD and directly associated with vascular calcification in CKD + Ca/P/VitD rats

Cortical bone volume and area were significantly reduced in both CKD groups as compared to CTL or CTL + Ca/P/VitD (Fig. 4), while cortical bone thickness was significantly reduced only in CKD + Ca/P/VitD rats as compared to the control groups. The reduced bone cortical thickness was also associated with lowered inner and outer cortical perimeter. In CKD + Ca/P/VitD group, bone cortical thickness, inner perimeter and cortical area were inversely correlated with vascular calcification (Online resource 3), which reinforces the current understanding that bone alterations occur simultaneously with vascular disease in CKD.

CKD + Ca/P/VitD rats have a low bone turnover and a mineralisation defect

In order to investigate the trabecular bone anomalies, we performed static and dynamic histomorphometry analysis both in primary and secondary spongiosa. Analysis of the secondary spongiosa showed that trabecular bone volume (BV/TV), thickness (TbTh) and number (TbN) were significantly increased in CKD rats with Ca/P/VitD as compared to the other groups ($p < 0.05$, Fig. 5). These changes in trabecular parameters were mainly associated with a significant increase in osteoid volume (OV/BV) and thickness (Oth) (Fig. 5). Dynamic bone parameters performed on trabecular bone revealed lower mineralisation surface, bone formation rate and mineral apposition rate in CKD + Ca/P/VitD rats, which confirms low bone turnover and mineralisation defect in this group (Table 2). Osteoclast number (OcN/BV), which reflects bone resorption activity, was also suppressed in CKD + Ca/P/VitD rats (Fig. 5). To better

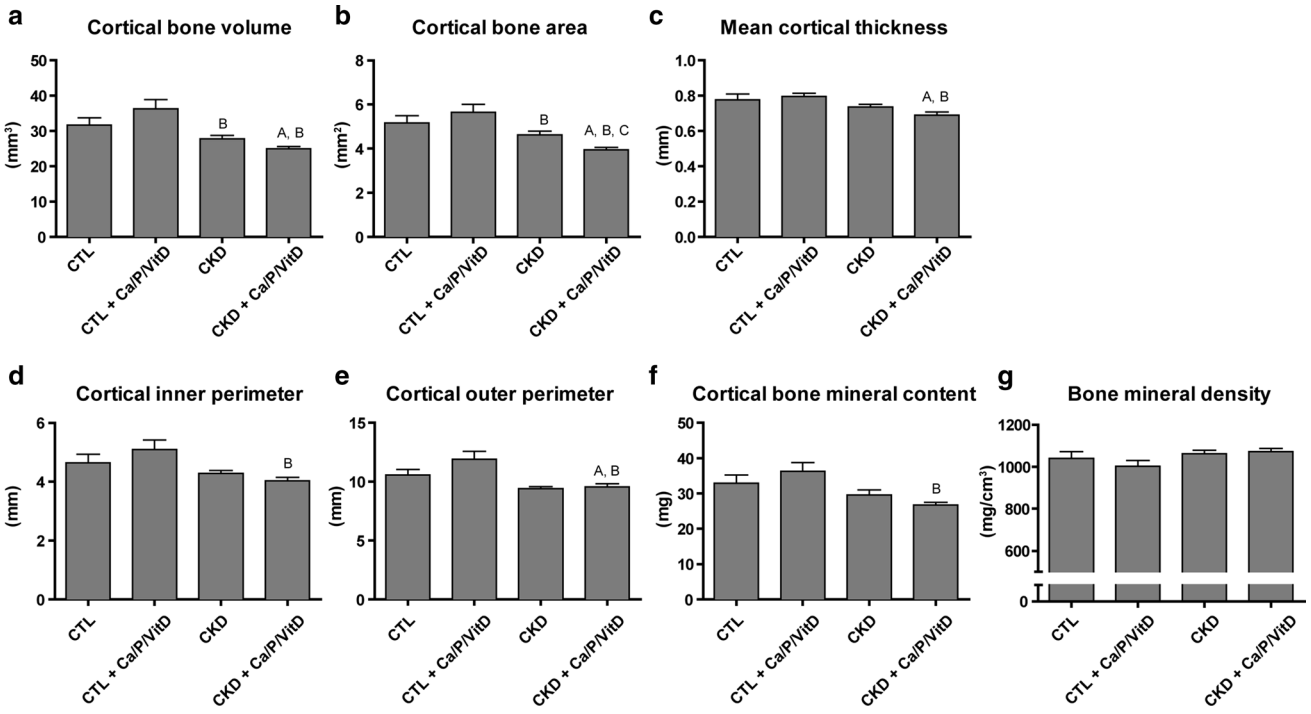

Fig. 4 Cortical parameters of tibia bone in the different groups. Cortical microarchitecture is significantly affected in chronic kidney disease rats with vascular calcification. *CKD* chronic kidney disease, *CTL* control, *Ca/P/VitD* calcium, phosphorus and vitamin D supplementation. A, $p < 0.05$ vs. CTL; B, $p < 0.05$ vs. CTL + Ca/P/VitD; C, $p < 0.05$ vs. CKD

characterize the bone anomalies in our growing rats, further analysis revealed significant accumulation of the trabecular primary spongiosa bone in CKD + Ca/P/VitD (0.958 ± 0.237 vs 0.123 ± 0.009 µm for CKD + normal diet) while the growth plate thickness was not different between groups (0.233 ± 0.005 vs 0.228 ± 0.022 µm in CKD vs CKD + Ca/P/VitD, respectively).

Bone expression of FGF-23 and DKK1, but not sclerostin and DMP1, is increased in CKD + Ca/P/VitD rats

Bone FGF23 mRNA levels were significantly higher in CKD + Ca/P/VitD as compared to control, while DKK1 expression was significantly higher in both CKD and CKD + Ca/P/VitD (Fig. 6). However, sclerostin and DMP1 mRNA levels in bone were comparable between groups.

Wnt signalling components in the bone

There were no differences in the bone transcription levels of Wnt ligands (WNT3A, WNT5A, WNT10B, WNT11), Fzd receptors (FZD1, FZD3, FZD7, FZD9) and AXIN2 between groups (Online resource 2). However, the degree of vascular calcification correlated with bone transcript levels of all investigated Wnt activators, namely WNT3A (*R* 0.667, $p = 0.042$), WNT5A (*R* 0.789, $p = 0.004$), WNT10 (*R* 0.642, $p = 0.033$) and WNT11 ($R = 0.642$, $p = 0.033$), and also with FZD3 transcript levels (*R* 0.780, $p = 0.005$).

Discussion

In the present study, we have used our established model of CKD rats with vascular calcification [20, 21] in order to study the expression of osteocyte markers and Wnt pathway proteins in the vessels as well as the anomalies of bone microarchitecture and mineralization. We found that: (1) Ca/P/VitD supplementation in CKD rats induced an osteocyte-like phenotype in the calcified vessels and changes in Wnt pathway activity; (2) CKD rats treated with Ca/P/VitD develop a mineralization defect, which may translate to higher bone fragility.

Due to the high prevalence of low bone turnover disease in CKD patients, a major concern about its association with vascular calcification has been raised [26]. In this study, despite lower PTH levels in control + Ca/P/VitD rats, the low bone remodeling state was observed only in CKD + Ca/P/VitD animals, which means that there is clearly a favorable environment in CKD that predisposes to low bone turnover. Sclerostin and DKK1, two soluble proteins that are highly expressed by the osteocytes and known to inhibit bone

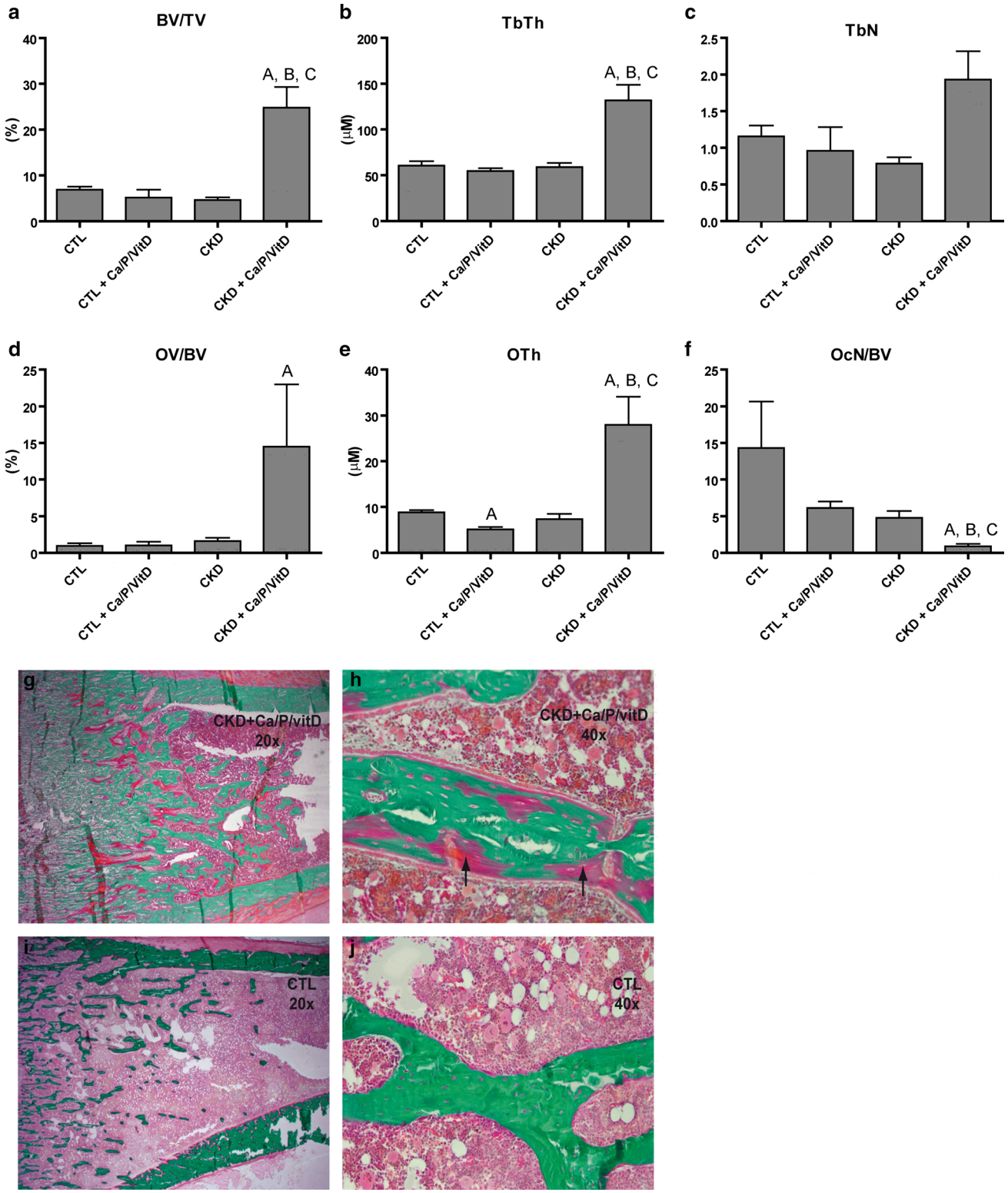

Fig. 5 Bone histomorphometry results and representative histological images of tibia bone. Histomorphometry analysis showed significantly increased trabecular bone volume (**a**), thickness (**b**), number (**c**), osteoid bone (**d**, **e**) and decreased osteoclasts number (**f**) in CKD + Ca/P/VitD rats. **g**, **h** CKD + Ca/P/VitD rats showing increased trabecular and osteoid (arrows) bone in primary and secondary spongiosa typical of mineralisation defect. **i**, **j** Control rats showing normal trabecular bone. Left panel: ×20 magnification; right panel: ×40 magnification. *CKD* chronic kidney disease, *CTL* control, *Ca/P/VitD* calcium, phosphorus and vitamin D supplementation, *BV/TV* bone volume/tissue volume, *TbTh* trabecular thickness, *TbN* trabecular number, *OV/BV* osteoid volume/bone volume, *OTh* osteoid thickness, *OcN/BV* osteoclast number/bone volume. A, $p < 0.05$ vs. CTL; B, $p < 0.05$ vs CTL + Ca/P/VitD; C, $p < 0.05$ vs CKD

Table 2 Bone dynamic parameters between groups

	CTL ($n=8$)	CTL + Ca/P/vitD ($n=8$)	CKD ($n=12$)	CKD + Ca/P/vitD ($n=12$)
MS/BS (%)	2.3 ± 1.2	7.5 ± 9.2	5.7 ± 1.5	1.3 ± 0.6
MAR (µm/day)	1.30 ± 0.21	1.40 ± 0.18	1.30 ± 0.44	0.63 ± 0.64
BFR-BS (mm^3/mm^2/year)	0.03 ± 0.02	0.09 ± 0.11	0.08 ± 0.05	0.01 ± 0.01
MS/OS (%)	11.0 ± 8.4	3.4 ± 0.1	8.2 ± 8.3	0.3 ± 0.3
sL/BS (%)	1.7 ± 0.5	4.8 ± 5.3	6.0 ± 1.7	1.7 ± 0.6
dL/BS (%)	1.2 ± 1.0	5.0 ± 6.4	2.6 ± 2.5	0.2 ± 0.3

Values are expressed as mean ± SD

CKD chronic kidney disease, *CTL* control, *Ca/P/VitD* calcium, phosphorus and vitamin D supplementation, *BFR-BS* bone formation rate-bone surface, *dL/BS* double label surface/bone surface, *MAR* mineralization apposition rate, *MS/BS* mineralization surface/bone surface, *MS/OS* mineralization surface/osteoid surface, *sL/BS* single label surface/bone surface

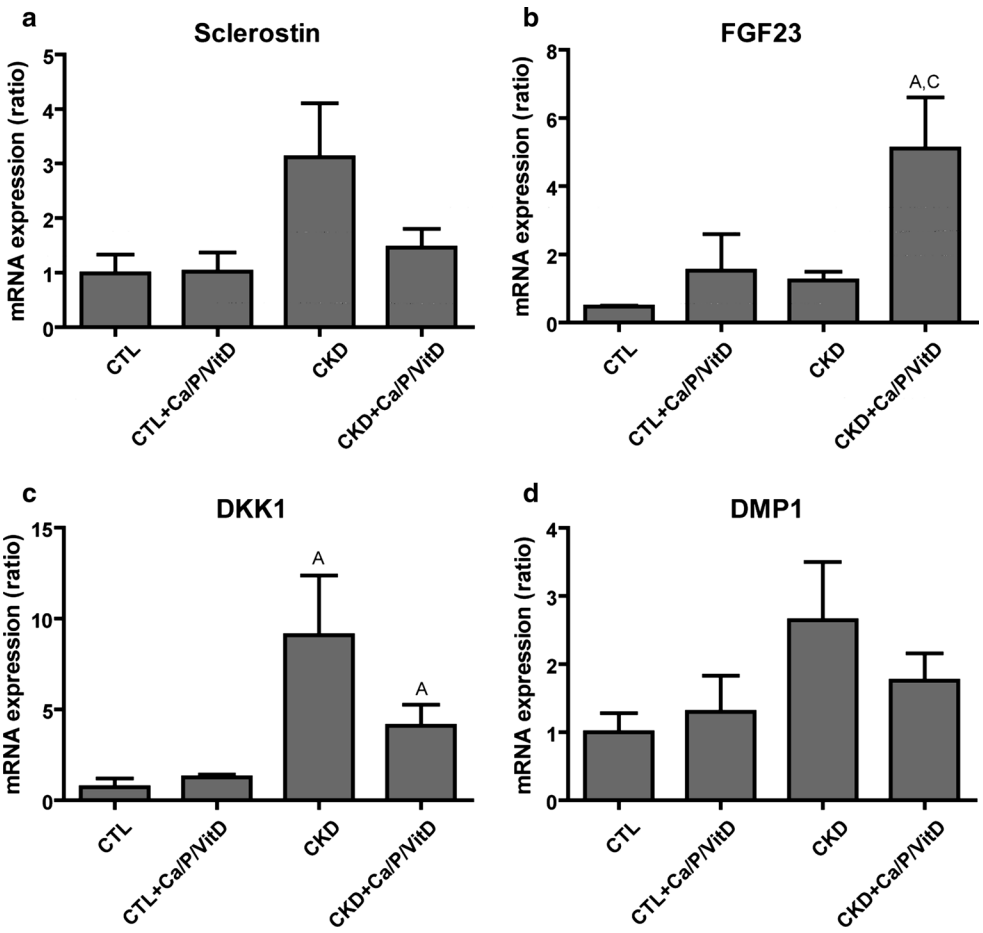

Fig. 6 mRNA expression of osteocytes markers in the femur. DKK1 transcription levels are significantly increased only in the CKD and CKD + Ca/P/VitD (**c**), while FGF23 transcription levels are only increased in the CKD + Ca/P/VitD group (**b**). Sclerostin and DMP1 gene expression appears to follow the same pattern as DKK1 but there is no significant difference between groups (**a**, **d**). *CKD* chronic kidney disease, *CTL* control, *Ca/P/VitD* calcium, phosphorus and vitamin D supplementation. A, C, $p < 0.05$ vs CTL and CKD, respectively

formation could contribute to the low bone turnover in CKD as their blood levels and vascular expression are increased only in CKD + Ca/P/VitD animals [27–29]. In accordance with the higher vascular levels of sclerostin and DKK1, the Wnt pathway appeared to be suppressed in the calcified vessels as phosphorylated GSK-3β (ser 9), which is inactive, was decreased, and Wnt target gene AXIN2 was less transcribed. Further findings that support a lowering of the Wnt activity in the calcified vessels are the negative correlations between vascular calcification and transcription of Wnt5A and Fzd7, respectively a Wnt activator and a Wnt receptor. Since activation of the Wnt pathway in the vessels has been shown to promote vascular calcification [30], sclerostin and DKK1 therefore seem to play a compensatory role to inhibit vascular calcification in CKD. It is worth mentioning that both total and phosphorylated β-catenin were also decreased

in calcified aorta from CKD + Ca/P/VitD animals, which at first view may suggest an upregulation of the Wnt pathway. However, we measured cytoplasmic β-catenin while measurement of the nuclear component would have been necessary to correctly interpret levels of β-catenin.

Interestingly, vascular expression of FGF23 was not increased in the group with extensive vascular calcification (CKD + Ca/P/VitD) despite a dramatically increased serum level. These findings suggest that FGF23 serum levels in CKD mainly originate from the bone and not from vessels. In contrast with our findings in the vessels, the bone tissue levels of sclerostin transcripts were not different as compared to control groups while DKK1 transcript levels were higher in CKD animals. These higher levels could be attributed to the high phosphate diet or to the elevated FGF23 levels, both having been associated with increased DKK1 production [31, 32]. As expected, the bone transcription of FGF23 was increased significantly in CKD + Ca/P/VitD animals. The positive correlation between vascular calcification and WNT3A, WNT5A, WNT10, WNT11 and FZD3 (five proteins involved in β-catenin stabilisation during vascular calcification) transcription in bone suggests a possible protective mechanism to avoid further bone deterioration by Wnt inhibitors in CKD. The fact that bone transcription of Axin2 was not increased in CKD + Ca/P/VitD animals suggests however that these changes may not be sufficient to increase Wnt/β-catenin activity.

In this study, cortical bone thickness, mineral content, and inner and outer perimeter were significantly decreased in CKD + Ca/P/VitD rats, which is likely the result of the calcitriol supplementation. Indeed, previous studies reported that treatment with calcitriol led to decreased cortical thickness and growth plate defects in non-CKD rats [33], and to growth alteration and reduced cortical thickness in CKD rats [34, 35]. In our study, bone turnover was actually low, suggesting that the cortical anomalies are likely due to defects in radial growth and not increased remodeling. With regards to the trabecular compartment and regardless of the effect of PTH, some studies have shown that calcium and/or calcitriol supplementation was associated with higher trabecular bone volume in different models of CKD and non-CKD rats [33, 36]. A particularly interesting observation in our study was the occurrence of bone mineralization defects in CKD + Ca/P/VitD rats, likely induced by the high dose of calcitriol supplementation. Wronski et al. have previously treated rats with daily calcitriol for 13 days and have found an accumulation of osteoid bone and prolongation of mineralization lag time [37]. These findings were recently confirmed by Lieben et al. who showed that calcitriol suppressed bone matrix mineralization by stimulating the transcription of genes encoding mineralisation inhibitors [38]. Finally, in a 5/6 nephrectomy model supplemented with calcitriol but not calcium, De Schutter et al. have also observed areas of impaired bone mineralization even though evident osteomalacia was not described [39]. Therefore, the combination of low PTH, high serum calcium and high-dose calcitriol seems deleterious to bone by inducing a mineralization defect despite lowering of bone turnover parameters. While calcitriol is widely used for the treatment of CKD-MBD [40], the beneficial effects of lowering PTH levels with calcitriol treatment on bone strength still remains to be proven [41, 42]. Future studies should therefore evaluate the direct role of osteocyte markers in the development of bone mineralization defects in CKD [43, 44].

Our study has limitations. First, we tried to replicate human CKD-MBD where calcitriol and calcium are frequently used in association. However, we recognize that the high dose of calcitriol used in our study as well as the phosphate supplementation are usually not given to CKD patients. The deleterious effect of calcitriol on bone mineralization is probably a matter of dose and further studies are necessary to better understand this. Secondly, CKD rats treated with Ca/P/VitD had a lower creatinine clearance than CKD rats not treated with Ca/P/VitD, which could have been related to the high phosphate diet. However, since the difference is only minimal, we do not think it may have influenced the results of our study. Finally, calcitriol supplementation has been previously reported to induce vascular calcification through upregulation of osteoblastic transcription factors in CKD animals [45]. Hence, it is always possible that the described vascular phenotype in our study has occurred independently of the bone turnover status when high dose calcitriol is given to induce vascular calcification.

In conclusion, we used calcium, phosphate and calcitriol to induce vascular calcification and low bone turnover in CKD rats to mimic CKD-MBD in humans. Our findings support the involvement of the Wnt pathway in vascular calcification and strengthen the importance of conducting studies to evaluate the bone effects of current treatments for CKD-MBD.

Acknowledgements Dr. Mac-Way holds a scholarship from FRQ-S (Grant no. 32661) and KRESCENT program from the CIHR-Kidney Foundation of Canada. This study was supported by a grant from the Kidney Foundation of Canada (Grant no. KFOC160013) and from the Department of Medicine and la Fondation du CHU de Québec from Université Laval. Dr. Agharazii holds a research chair in nephrology from Université Laval.

Author contributions MA, RL and FMW conceived and designed the study. SKB and FMW performed the statistical analyses. SKB, DV and RVU conducted animal experimentations, tissue specimens handling, and interpreted the findings. SP and FMW were in charge of the bone histomorphometry analysis. SKB and FMW wrote the first draft and revised all subsequent versions. All authors provided their input, expertise and critical review of the paper. All authors read and approved the final version of the paper. FMW had full access to the data and takes responsibility for the integrity and accuracy of the data analysis.

Compliance with ethical standards

Conflict of interest All authors have no conflicts of interest.

References

1. (2009) KDIGO clinical practice guideline for the diagnosis, evaluation, prevention, and treatment of chronic kidney disease-mineral and bone disorder (CKD-MBD). Kidney Int Suppl S1–S130 https://doi.org/10.1038/ki.2009.188
2. Cozzolino M, Urena-Torres P, Vervloet MG, Brandenburg V, Bover J, Goldsmith D, Larsson TE, Massy ZA, Mazzaferro S, ERA-EDTA C-MWGo (2014) Is chronic kidney disease-mineral bone disorder (CKD-MBD) really a syndrome? Nephrol Dial Transplant 29:1815–1820. https://doi.org/10.1093/ndt/gft514
3. Shanahan CM, Cary NR, Salisbury JR, Proudfoot D, Weissberg PL, Edmonds ME (1999) Medial localization of mineralization-regulating proteins in association with Monckeberg's sclerosis: evidence for smooth muscle cell-mediated vascular calcification. Circulation 100:2168–2176
4. Goodman WG, London G, Amann K, Block GA, Giachelli C, Hruska KA, Ketteler M, Levin A, Massy Z, McCarron DA, Raggi P, Shanahan CM, Yorioka N, Vascular Calcification Work G (2004) Vascular calcification in chronic kidney disease. Am J Kidney Dis 43:572–579
5. Stehman-Breen C (2004) Osteoporosis and chronic kidney disease. Semin Nephrol 24:78–81
6. Nickolas TL, Stein E, Cohen A, Thomas V, Staron RB, McMahon DJ, Leonard MB, Shane E (2010) Bone mass and microarchitecture in CKD patients with fracture. J Am Soc Nephrol 21:1371–1380. https://doi.org/10.1681/ASN.2009121208
7. Foley RN, Parfrey PS, Sarnak MJ (1998) Epidemiology of cardiovascular disease in chronic renal disease. J Am Soc Nephrol 9:S16–S23
8. Watanabe R, Lemos MM, Carvalho AB, Rochitte CE, Santos RD, Draibe SA, Canziani ME (2012) The association between coronary artery calcification progression and loss of bone density in non-dialyzed CKD patients. Clin Nephrol 78:425–431. https://doi.org/10.5414/CN107515
9. Toussaint ND, Lau KK, Strauss BJ, Polkinghorne KR, Kerr PG (2008) Associations between vascular calcification, arterial stiffness and bone mineral density in chronic kidney disease. Nephrol Dial Transplant 23:586–593. https://doi.org/10.1093/ndt/gfm660
10. Hak AE, Pols HA, van Hemert AM, Hofman A, Witteman JC (2000) Progression of aortic calcification is associated with metacarpal bone loss during menopause: a population-based longitudinal study. Arterioscler Thromb Vasc Biol 20:1926–1931
11. Drueke TB, Massy ZA (2016) Changing bone patterns with progression of chronic kidney disease. Kidney Int 89:289–302. https://doi.org/10.1016/j.kint.2015.12.004
12. Andress DL (2008) Adynamic bone in patients with chronic kidney disease. Kidney Int 73:1345–1354. https://doi.org/10.1038/ki.2008.60
13. Malluche HH, Monier-Faugere MC (1992) Risk of adynamic bone disease in dialyzed patients. Kidney Int Suppl 38:S62–S67
14. London GM, Marty C, Marchais SJ, Guerin AP, Metivier F, de Vernejoul MC (2004) Arterial calcifications and bone histomorphometry in end-stage renal disease. J Am Soc Nephrol 15:1943–1951
15. Frazao JM, Martins P (2009) Adynamic bone disease: clinical and therapeutic implications. Curr Opin Nephrol Hypertens 18:303–307. https://doi.org/10.1097/MNH.0b013e32832c4df0
16. Pelletier S, Dubourg L, Carlier MC, Hadj-Aissa A, Fouque D (2013) The relation between renal function and serum sclerostin in adult patients with CKD. Clin J Am Soc Nephrol 8:819–823. https://doi.org/10.2215/CJN.07670712
17. Ferreira JC, Ferrari GO, Neves KR, Cavallari RT, Dominguez WV, Dos Reis LM, Graciolli FG, Oliveira EC, Liu S, Sabbagh Y, Jorgetti V, Schiavi S, Moyses RM (2013) Effects of dietary phosphate on adynamic bone disease in rats with chronic kidney disease—role of sclerostin? PLoS One 8:e79721. https://doi.org/10.1371/journal.pone.0079721PONE-D-13-17719
18. de Oliveira RA, Barreto FC, Mendes M, dos Reis LM, Castro JH, Britto ZM, Marques ID, Carvalho AB, Moyses RM, Jorgetti V (2015) Peritoneal dialysis per se is a risk factor for sclerostin-associated adynamic bone disease. Kidney Int 87:1039–1045. https://doi.org/10.1038/ki.2014.372
19. Bover J, Urena P, Brandenburg V, Goldsmith D, Ruiz C, DaSilva I, Bosch RJ (2014) Adynamic bone disease: from bone to vessels in chronic kidney disease. Semin Nephrol 34:626–640. https://doi.org/10.1016/j.semnephrol.2014.09.008
20. Gauthier-Bastien A, Ung RV, Lariviere R, Mac-Way F, Lebel M, Agharazii M (2013) Vascular remodeling and media calcification increases arterial stiffness in chronic kidney disease. Clin Exp Hypertens. https://doi.org/10.3109/10641963.2013.804541
21. Agharazii M, St-Louis R, Gautier-Bastien A, Ung RV, Mokas S, Lariviere R, Richard DE (2015) Inflammatory cytokines and reactive oxygen species as mediators of chronic kidney disease-related vascular calcification. Am J Hypertens 28:746–755. https://doi.org/10.1093/ajh/hpu225
22. Pfaffl MW (2001) A new mathematical model for relative quantification in real-time RT-PCR. Nucleic Acids Res 29:e45
23. Chappard D, Palle S, Alexandre C, Vico L, Riffat G (1987) Bone embedding in pure methyl methacrylate at low temperature preserves enzyme activities. Acta Histochem 81:183–190. https://doi.org/10.1016/S0065-1281(87)80012-0
24. Parfitt AM, Drezner MK, Glorieux FH, Kanis JA, Malluche H, Meunier PJ, Ott SM, Recker RR (1987) Bone histomorphometry: standardization of nomenclature, symbols, and units. Report of the ASBMR Histomorphometry Nomenclature Committee. J Bone Miner Res 2:595–610. https://doi.org/10.1002/jbmr.5650020617
25. Dempster DW, Compston JE, Drezner MK, Glorieux FH, Kanis JA, Malluche H, Meunier PJ, Ott SM, Recker RR, Parfitt AM (2013) Standardized nomenclature, symbols, and units for bone histomorphometry: a 2012 update of the report of the ASBMR Histomorphometry Nomenclature Committee. J Bone Miner Res 28:2–17. https://doi.org/10.1002/jbmr.1805
26. Moe SM (2006) Vascular calcification and renal osteodystrophy relationship in chronic kidney disease. Eur J Clin Investig 36:51–62. https://doi.org/10.1111/j.1365-2362.2006.01665.x
27. Vervloet MG, Massy ZA, Brandenburg VM, Mazzaferro S, Cozzolino M, Urena-Torres P, Bover J, Goldsmith D, ERA-EDTA C-MWGo (2014) Bone: a new endocrine organ at the heart of chronic kidney disease and mineral and bone disorders. Lancet Diabetes Endocrinol 2:427–436. https://doi.org/10.1016/S2213-8587(14)70059-2
28. Brandenburg VM, D'Haese P, Deck A, Mekahli D, Meijers B, Neven E, Evenepoel P (2015) From skeletal to cardiovascular disease in 12 steps—the evolution of sclerostin as a major player in CKD-MBD. Pediatr Nephrol. https://doi.org/10.1007/s00467-015-3069-7
29. Burgers TA, Williams BO (2013) Regulation of Wnt/beta-catenin signaling within and from osteocytes. Bone 54:244–249. https://doi.org/10.1016/j.bone.2013.02.022
30. Cai T, Sun D, Duan Y, Wen P, Dai C, Yang J, He W (2016) WNT/beta-catenin signaling promotes VSMCs to osteogenic transdifferentiation and calcification through directly modulating

Runx2 gene expression. Exp Cell Res 345:206–217. https://doi.org/10.1016/j.yexcr.2016.06.007
31. Ferreira JC, Ferrari GO, Neves KR, Cavallari RT, Dominguez WV, dos Reis LM, Graciolli FG, Oliveira EC, Liu SG, Sabbagh Y, Jorgetti V, Schiavi S, Moyses RMA (2013) Effects of dietary phosphate on adynamic bone disease in rats with chronic kidney disease—role of sclerostin? PLoS One 8:7. https://doi.org/10.1371/journal.pone.0079721
32. Carrillo-Lopez N, Panizo S, Alonso-Montes C, Roman-Garcia P, Rodriguez I, Martinez-Salgado C, Dusso AS, Naves M, Cannata-Andia JB (2016) Direct inhibition of osteoblastic Wnt pathway by fibroblast growth factor 23 contributes to bone loss in chronic kidney disease. Kidney Int 90:77–89. https://doi.org/10.1016/j.kint.2016.01.024
33. Idelevich A, Kerschnitzki M, Shahar R, Monsonego-Ornan E (2011) 1,25(OH)(2)D-3 alters growth plate maturation and bone architecture in young rats with normal renal function. PLoS One 6:14. https://doi.org/10.1371/journal.pone.0020772
34. Hopper TAJ, Wehrli FW, Saha PK, Andre JB, Wright AC, Sanchez CP, Leonard MB (2007) Quantitative microcomputed tomography assessment of intratrabecular, intertrabecular, and cortical bone architecture in a rat model of severe renal osteodystrophy. J Comput Assist Tomogr 31:320–328. https://doi.org/10.1097/01.rct.0000238007.19258.3d
35. Parfitt AM (1997) The hyperparathyroidism of chronic renal failure: a disorder of growth. Kidney Int 52:3–9. https://doi.org/10.1038/ki.1997.297
36. Diaz MN, Rodriguez AR, Martin JLF, Arias MS, Rodriguez PM, Cannata Andia JB (2007) Effects of estradiol, calcitriol and both treatments combined on bone histomorphometry in rats with chronic kidney disease and ovariectomy. Bone 41:614–619. https://doi.org/10.1016/j.bone.2007.06.026
37. Wronski TJ, Halloran BP, Bikle DD, Globus RK, Morey-Holton ER (1986) Chronic administration of 1,25-dihydroxyvitamin D3: increased bone but impaired mineralization. Endocrinology 119:2580–2585. https://doi.org/10.1210/endo-119-6-2580
38. Lieben L, Masuyama R, Torrekens S, Van Looveren R, Schrooten J, Baatsen P, Lafage-Proust MH, Dresselaers T, Feng JQ, Bonewald LF, Meyer MB, Pike JW, Bouillon R, Carmeliet G (2012) Normocalcemia is maintained in mice under conditions of calcium malabsorption by vitamin D-induced inhibition of bone mineralization. J Clin Investig 122:1803–1815. https://doi.org/10.1172/JCI45890
39. De Schutter TM, Behets GJ, Jung S, Neven E, D'Haese PC, Querfeld U (2012) Restoration of bone mineralization by cinacalcet is associated with a significant reduction in calcitriol-induced vascular calcification in uremic rats. Calcif Tissue Int 91:307–315. https://doi.org/10.1007/s00223-012-9635-0
40. Wesseling-Perry K, Salusky IB (2013) Chronic kidney disease: mineral and bone disorder in children. Semin Nephrol 33:169–179. https://doi.org/10.1016/j.semnephrol.2012.12.017
41. Newman CL, Tian N, Hammond MA, Wallace JM, Brown DM, Chen NX, Moe SM, Allen MR (2016) Calcitriol suppression of parathyroid hormone fails to improve skeletal properties in an animal model of chronic kidney disease. Am J Nephrol 43:20–31. https://doi.org/10.1159/000444423
42. Fortier C, Mac-Way F, De Serres SA, Marquis K, Douville P, Desmeules S, Lariviere R, Agharazii M (2014) Active vitamin D and accelerated progression of aortic stiffness in hemodialysis patients: a longitudinal observational study. Am J Hypertens 27:1346–1354. https://doi.org/10.1093/ajh/hpu057
43. Atkins GJ, Rowe PS, Lim HP, Welldon KJ, Ormsby R, Wijenayaka AR, Zelenchuk L, Evdokiou A, Findlay DM (2011) Sclerostin is a locally acting regulator of late-osteoblast/preosteocyte differentiation and regulates mineralization through a MEPE-ASARM-dependent mechanism. J Bone Miner Res 26:1425–1436. https://doi.org/10.1002/jbmr.345
44. Shalhoub V, Ward SC, Sun B, Stevens J, Renshaw L, Hawkins N, Richards WG (2011) Fibroblast growth factor 23 (FGF23) and alpha-klotho stimulate osteoblastic MC3T3.E1 cell proliferation and inhibit mineralization. Calcif Tissue Int 89:140–150. https://doi.org/10.1007/s00223-011-9501-5
45. Jung S, Querfeld U, Muller D, Rudolph B, Peters H, Kramer S (2012) Submaximal suppression of parathyroid hormone ameliorates calcitriol-induced aortic calcification and remodeling and myocardial fibrosis in uremic rats. J Hypertens 30:2182–2191. https://doi.org/10.1097/HJH.0b013e328357c049